ACCOUNTS of chemical research

Article

pubs.acs.org/accounts

Rotaxane-Based Molecular Muscles

Carson J. Bruns and J. Fraser Stoddart*

Department of Chemistry, Northwestern University, 2145 Sheridan Road, Evanston, Illinois 60201-3113, United States

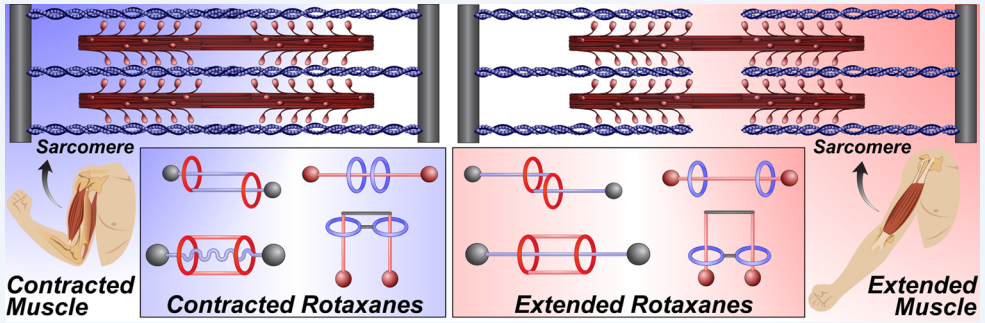

CONSPECTUS: More than two decades of investigating the chemistry of bistable mechanically interlocked molecules (MIMs), such as rotaxanes and catenanes, has led to the advent of numerous molecular switches that express controlled translational or circumrotational movement on the nanoscale. Directed motion at this scale is an essential feature of many biomolecular assemblies known as molecular machines, which carry out essential life-sustaining functions of the cell. It follows that the use of bistable MIMs as artificial molecular machines (AMMs) has been long anticipated. This objective is rarely achieved, however, because of challenges associated with coupling the directed motions of mechanical switches with other systems on which they can perform work.

A natural source of inspiration for designing AMMs is muscle tissue, since it is a material that relies on the hierarchical organization of molecular machines (myosin) and filaments (actin) to produce the force and motion that underpin locomotion, circulation, digestion, and many other essential life processes in humans and other animals. Muscle is characterized at both microscopic and macroscopic length scales by its ability to generate forces that vary the distance between two points at the expense of chemical energy. Artificial muscles that mimic this ability are highly sought for applications involving the transduction of mechanical energy. Rotaxane-based molecular switches are excellent candidates for artificial muscles because their architectures intrinsically possess movable filamentous molecular components. In this Account, we describe (i) the different types of rotaxane "molecular muscle" architectures that express contractile and extensile motion, (ii) the molecular recognition motifs and corresponding stimuli that have been used to actuate them, and (iii) the progress made on integrating and scaling up these motions for potential applications. We identify three types of rotaxane muscles, namely, "daisy chain", "press", and "cage" rotaxanes, and discuss their mechanical actuation driven by ions, pH, light, solvents, and redox stimuli. Different applications of these rotaxane-based molecular muscles are possible at various length scales. On a molecular level, they have been harnessed to create adjustable receptors and to control electronic communication between chemical species. On the mesoscale, they have been incorporated into artificial muscle materials that amplify their concerted motions and forces, making future applications at macroscopic length scales look feasible.

We emphasize how rotaxanes constitute a remarkably versatile platform for directing force and motion, owing to the wide range of stimuli that can be used to actuate them and their diverse modes of mechanical switching as dictated by the stereochemistry of their mechanical bonds, that is, their mechanostereochemistry. We hope that this Account will serve as an exposition that sets the stage for new applications and materials that exploit the capabilities of rotaxanes to transduce mechanical energy and help in paving the path going forward to genuine AMMs.

■ INTRODUCTION

Molecular nanotechnology, which involves the precise manipulation of matter at atomic and molecular scales, has been mastered by Nature over billions of years of evolution. A vast and dazzling network[1] of dynamic, self-assembled nanostructures maintain the cell, the building block of life. Among the most important nanotechnologies at the cell's disposal are molecular machines,[2] biomolecular assemblies that transduce chemical and mechanical energy to perform vital cell functions. Molecular machines are involved,[3] for example, in gene replication (e.g., DNA and RNA polymerases), protein synthesis (ribosomes), synthesizing the cell's energy currency (ATP synthase), transporting intracellular cargo (e.g., kinesin and dynein), and locomotion (e.g., flagella and myosin). These enzymes and motor proteins serve as a source of inspiration for the design of synthetic compounds as artificial molecular machines[4−6] (AMMs).

Fundamentally, AMMs must convert an input of energy into a mechanical output, or vice versa. This basic requirement is why

Special Issue: Responsive Host−Guest Systems

Received: March 31, 2014
Published: May 30, 2014

   dx.doi.org/10.1021/ar500138u | Acc. Chem. Res. 2014, 47, 2186−2199

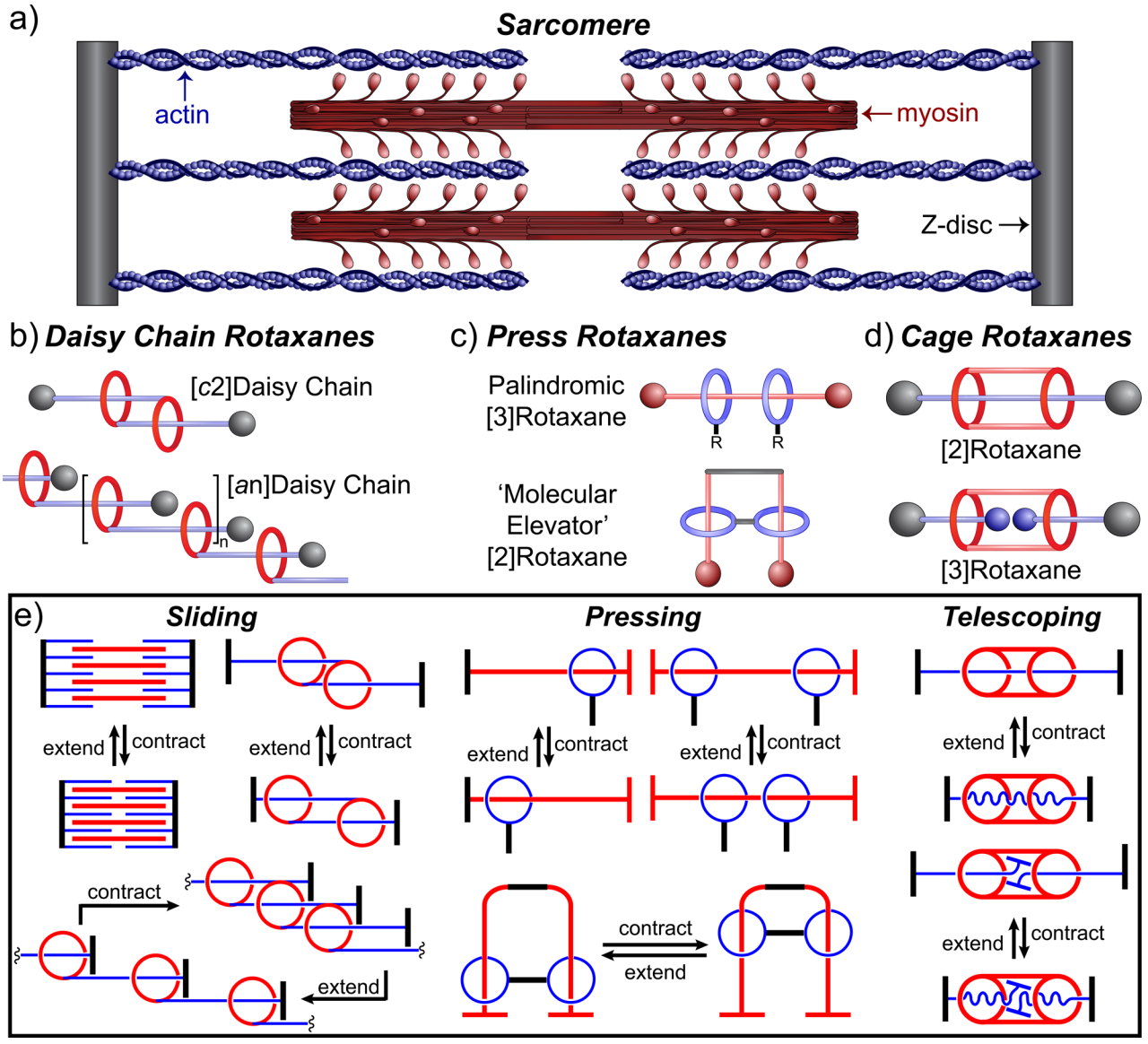

Figure 1. Comparison between the structures of (a) the sarcomere and (b–d) rotaxane-based molecular muscles. (e) Graphical representations of the contractile motions of natural and rotaxane-based muscle architectures. Sarcomeres (top, left) contract by shortening the distance between Z-discs (black) through the antiparallel sliding of myosin (red) and actin (blue) filaments. The rotaxanes are color-coded to reflect which of their components assume the same roles as their natural counterparts.

mechanically interlocked molecules[7] (MIMs), such as catenanes and rotaxanes, have been frequently targeted and marketed as potential AMMs. MIMs possess molecular components that are linked only by mechanical bonds, restricting their freedom of motion except along certain well-defined pathways. We refer to the stereochemistry of MIMs as mechanostereochemistry.[8] Mechanostereochemical isomerism is often exploited to control bistable [2]catenanes that express circumrotational motion of their interlocked rings or [2]rotaxanes that express translational motion of their rings along their associated dumbbells. These ring displacements are driven by biased Brownian motion, resulting from an external stimulus that influences local noncovalent interactions. Although bistable switches are commonplace in the literature, the vast majority of them are not machines because they are not used to perform work.

The challenge of coaxing molecular switches into doing work[6,9] has been met only rarely, most often by incorporating them into materials that scale up their motions, for example, photodriven molecular rotors embedded in liquid crystal films driving the rotation of glass rods,[10] monolayers of photoswitchable rotaxanes transporting small droplets on surfaces,[11] and photoisomerizable moieties in liquid crystal elastomers driving the translational motion of pulleys[12] or magnets.[13] A naturally occurring scale-up of work done by molecular machines is manifest (Figure 1) in muscle tissue. Several artificial muscle materials have emerged, but they are typically polymers[14] that express bulk volume changes driven by electrostatic forces,[15] ion-solvation effects,[16,17] or thermal transitions,[18] rather than the synchronized motions of molecular machines, whereas artificial muscles that do amplify molecular motions are based on photoisomerizable compounds[19] such as azobenzene[20,21] and diarylethenes.[22] Thus, the repertoire of available stimuli for actuating biomimetic artificial muscles remains limited. Bistable rotaxanes have potential to diversify and improve the functions of soft artificial muscles, since (i) they can be implemented on virtually any length scale because their actuation is realized at

dx.doi.org/10.1021/ar500138u | Acc. Chem. Res. 2014, 47, 2186–2199

the single-molecule level, (ii) their actuation can supply a diverse set of well-defined mechanical motions dictated by their mechanostereochemistry, and (iii) they can be controlled by a wide variety of energy sources,[23] including light, acids/bases, cations, anions, reagents, and solvents, as well as by mechanical, thermal, or electrochemical stimuli.

This Account chronicles the development of a variety of bistable, rotaxane-based "molecular muscles" whose extensile and contractile motions are enabled by mechanical bonds and progress on their integration into nanomechanical systems at various length scales. We offer "bare essentials" descriptions of (i) three classes of rotaxane-based muscle architectures, (ii) the structural motifs and energy sources used to actuate them, and (iii) strategies that have emerged to couple, integrate, and scale up their mechanical motions.

■ ARCHITECTURES OF ROTAXANE MUSCLES

The repeating units of muscle tissue responsible for producing force and motion are sarcomeres (Figure 1a). The contractions of sarcomeres involve motor proteins that decorate filaments of myosin, which hydrolyze ATP to release energy that fuels a mechanical bending process. The myosin heads "pull" on interdigitated filaments of actin during the calcium-triggered exposure of their myosin binding sites. The resulting antiparallel sliding of myosin and actin filaments causes the end points of the sarcomere (Z-discs) to move closer together because they contain capping proteins that connect them to the filaments.

Molecular architectures that mimic sarcomeres can be defined by conceptually substituting their basic components (myosin, actin, Z-discs) for the componentry (rings, threads, stoppers) of rotaxanes. We identify three types of architectures in Figure 1, "daisy chain", "press", and "cage" rotaxanes, with potential to serve as molecular muscles. Daisy chains[24] (Figure 1b) comprise covalently linked, self-complementary ring−thread monomers, which are cross-threaded into cyclic or acyclic oligomers. [*c*2]Daisy chains, for example, are cyclic dimers in which mechanical bonds allow each monomer to slide past its partner in one dimension. Thus, a daisy chain's stoppers represent Z-discs, while the threads' sliding motions imitate those of actin and myosin. Several architectures encompass press rotaxanes (Figure 1c). Multicomponent "palindromic" rotaxanes involve controlled ring movements that oppose one another by virtue of a plane of symmetry through the center of the dumbbell(s). These mirror-image motions resemble those of a machine press. In these rotaxanes, the rings assume the role of Z-disc-bearing actin filaments and the dumbbells represent stationary myosin fibers. "Molecular elevators" are another class of press rotaxanes, in which a multivalent platform of rings passes between different sites of a multivalent thread/stopper component. Even simple [2]rotaxanes can act as presses by appropriately designating one "Z-disc" on the thread and another on the ring. Another rotaxane-based muscle architecture (Figure 1d) is based on cage-like hosts rather than rings. Cage rotaxanes can express telescoping motions, which resemble those of objects with concentric tubular parts such as hydraulic lifts and extendable antennae. The telescopic contraction of a cage rotaxane is accomplished by compressing one or more thread/stopper "dumbbells" (representing the actin/Z-disc components) within the cage's cavity. These rotaxanes' contractile motions are compared in Figure 1e, where the components that assume the functional roles of actin, myosin, and Z-discs are colored in blue, red, and black, respectively.

■ ION-DRIVEN SWITCHING

The imitation of sarcomere function in rotaxanes was pioneered[25−27] by Sauvage's group, who used transition metal ion templates to expand and contract (Scheme 1) the molecular length of a [*c*2]daisy chain. The rings of the daisy chain contain bidentate phenanthroline ligands, while the corresponding threads bear bidentate phenanthroline and tridentate terpyridine ligands. The pairing of ring and thread ligands around different templates affords different coordination geometries determined by the valency of the transition metal. The phenanthroline ligands of each component pair up tetrahedrally around Cu^{I} ions, rendering an extended geometry for $\mathbf{1Cu_2}^{2+}$. By contrast, Zn^{II} templates get sequestered in a pentacoordinate complex involving terpyridine ligands, furnishing a contracted geometry for $\mathbf{1Zn_2}^{4+}$. The muscle-like actuation between these two coconformations goes through a nonmetalated intermediate, which is generated by stripping out the metal templates with an excess of cyanide ligands.

The Sauvage group has also developed[28] "press" rotaxanes that are actuated by the addition and removal of transition metal ions. Compound **2**[29,30] is a cyclic [4]rotaxane, comprising two rigid bis(triazolylbipyridine) dumbbells and two porphyrin-based phenanthrolic bis-macrocycles, which contracts and expands (Scheme 2) in a unique manner. In the presence of Cu^{I} templates, $\mathbf{2Cu_4}^{4+}$ adopts a rigid square-shaped geometry held together at its corners by tetrahedral complexes formed between the bidentate ligands in each component. Demetalation with KCN collapses the structure of **2**, where one triazole group from each dumbbell coordinates axially to the zinc porphyrin center of a bis-macrocycle, leading to an estimated 2.7 nm contraction in molecular diameter.

Chiu and co-workers have reported[31] a cage [2]rotaxane, $\mathbf{3}^{4+}$, that telescopes (Scheme 3) under the influence of anion exchange. The cage comprises two [24]crown-8 rings joined by rigid triptycene linkers. The thread possesses secondary dialkylammonium and pyridinium sites, both of which can be stabilized by the crown ethers through hydrogen bonding interactions. As the tetrafluoroborate salt, the dumbbell of **3**·$4BF_4$ is fully extended such that the crown ethers predominantly encircle the ammonium sites. Upon the addition of fluoride, however, strong ammonium−fluoride ion-pairing interactions outcompete the stabilizing effect of the crown ethers, causing the dumbbell to compress within the cage such that its crown ethers preferentially encircle the pyridinium units in **3**·4F. This telescoping motion supplies ∼1.5 nm of stopper-to-stopper contraction.

■ pH-DRIVEN SWITCHING

The recognition motif between secondary dialkylammonium salts and crown ethers (as in compound **3**) is often exploited to create rotaxanes that respond to pH changes, since deprotonating the ammonium groups reduces the strength of their hydrogen bonding interactions. These switches are commonly designed with permanent cations as secondary stations, which displace the neutral amines within the rings under basic conditions. We have implemented this strategy (Figure 2) in two types of molecular muscles. The triply interlocked "molecular elevator",[32,33] $\mathbf{4H_3}^{9+}$, relies on pH to control (Figure 2a) the distance between two molecular platforms. Three crown ethers fused trigonally to an aromatic core are interlocked with a trifurcated "rig" component with two cationic recognition sites, dialkylammonium ($-NH_2^+-$) and 4,4′-bipyridinium ($BIPY^{2+}$), on each of its three legs. The crown ethers of the mobile platform encircle the

dx.doi.org/10.1021/ar500138u | *Acc. Chem. Res.* 2014, 47, 2186−2199

Scheme 1. Actuation of [*c*2]Daisy Chain $1Cu_2^{2+}/1Zn_2^{4+}$ Using Transition Metal Ion Exchange

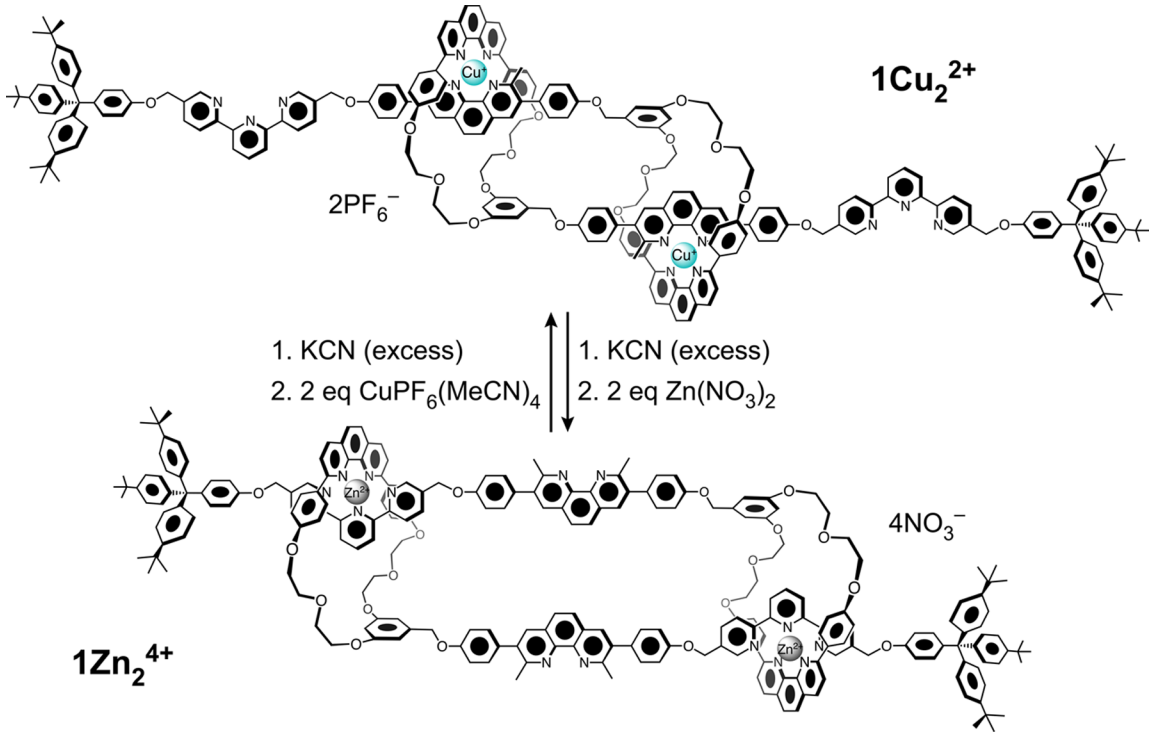

Scheme 2. Actuation of Cyclic [4]Rotaxane $2Cu_4^{4+}/2$, Which Collapses and Expands upon Demetalation and Remetalation, Respectively

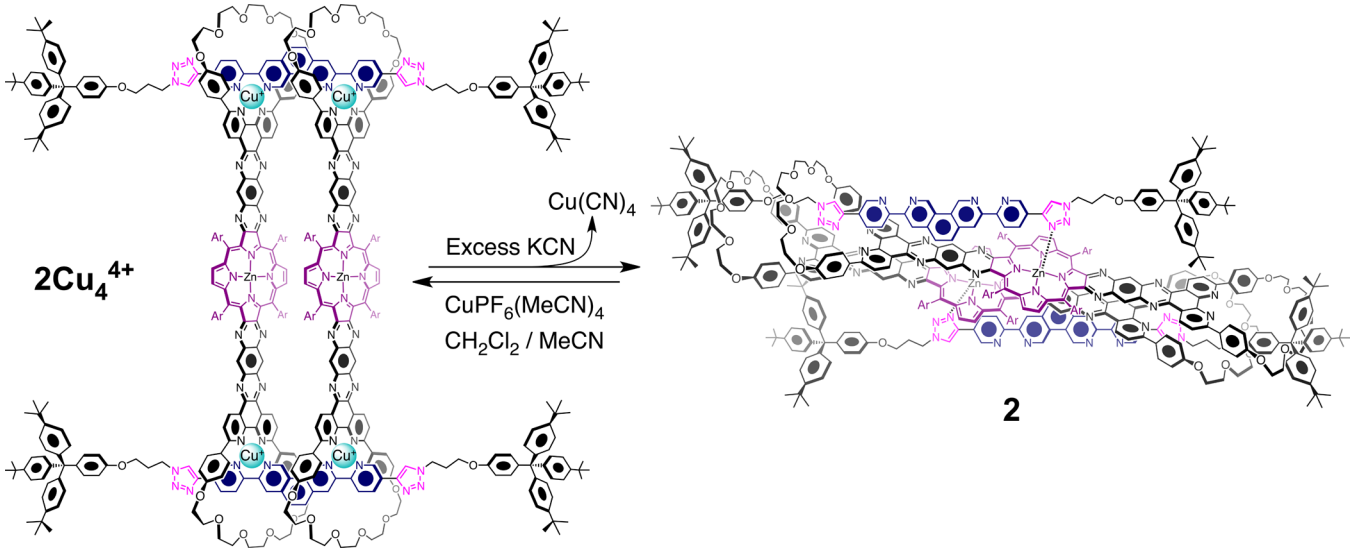

$-NH_2^+-$ sites with >99.9% selectivity in $\mathbf{4H_3}^{9+}$. Deprotonation of $-NH_2^+-$ with a phosphazine base causes the platform to migrate ~0.7 nm away to allow its benzo[24]crown-8 rings to stabilize the $BIPY^{2+}$ units via hydrogen bonding and π-associated donor−acceptor interactions in $\mathbf{4}^{6+}$. The flexibility of the rig allows this process to occur in a stepwise manner, rather than by the concerted movement of all three rings. It has been estimated[32] from a thermodynamic analysis that this mechanical stroke could generate up to 200 pN of force. Restoring the $-NH_2^+-$ sites with trifluoroacetic acid returns the platform to its original position. The same design motif was subsequently incorporated into [*c*2]daisy chain $\mathbf{5H_2}^{6+}$,[34] which expands and contracts (Figure 2b) using the same chemistry.

Other pH-switchable rotaxane-based molecular muscles are depicted in Figure 3. The Coutrot group independently reported[35] on a pH-switchable [*c*2]daisy chain at the same time as us.[33] Their compound $\mathbf{6H_2}^{4+}$ operates analogously to $\mathbf{5H_2}^{4+}$, except that it utilizes a triazolium unit as the permanent cation. Rotaxanes $\mathbf{7H_2}^{4+}$, $\mathbf{8H_2}^{4+}$, and $\mathbf{9H_2}^{4+}$ also employ dialkylammonium/triazolium motifs. Liu's group[36,37] prepared rotaxanes $\mathbf{7H_2}^{4+}$ and $\mathbf{8H_2}^{4+}$, which utilize identical dumbbell components in palindromic [3]rotaxanes and doubly interlocked molecular elevators, respectively. Chen and co-workers[38] described the cage [3]rotaxane $\mathbf{9H_2}^{4+}$ and its novel telescoping behavior. Other pH-switchable palindromic [3]rotaxanes that could be adapted for muscle-like functions have been developed

dx.doi.org/10.1021/ar500138u | *Acc. Chem. Res.* 2014, 47, 2186−2199

Scheme 3. Counterion Exchange between the Tetrafluoroborate and Fluoride Salts of Cage [2]Rotaxane 3^{4+} Results in Telescoping Motions That Expand and Compress the Dumbbell, Resulting from Differences in the Corresponding Ion-Pairing Interactions with the Dumbbell's Dialkylammonium Groups

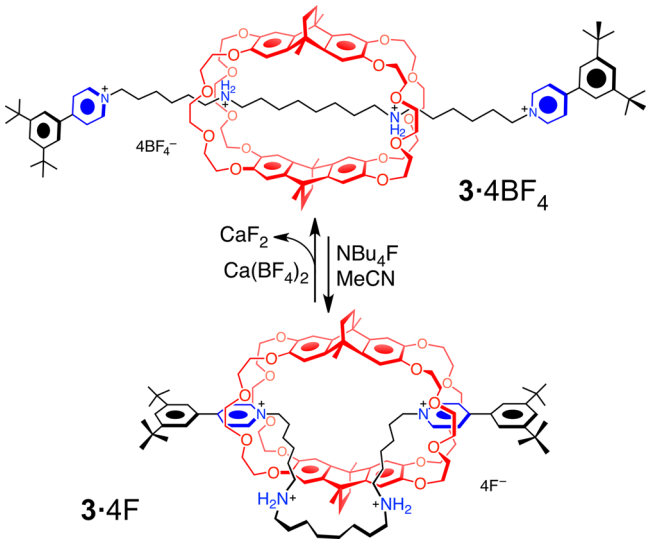

in the groups of Tuncel,[39,40] Takata,[41] Li,[42] and Tokunaga and Hisada.[43]

PHOTOCHEMICAL SWITCHING

Light is an attractive source of energy for powering molecular machines because it can be delivered rapidly, without generating waste products, while providing a means of monitoring the system.[44] Figure 4 portrays three photoswitchable [*c*2]daisy chains, all of them utilizing α-cyclodextrin (α-CD) derivatives as the macrocyclic components,in which the $E \rightarrow Z$ photoisomerization of a photoactive guest leads to its extrusion from α-CD and concomitant molecular contraction. This strategy was demonstrated (Figure 4a) in Kaneda's group[45] using compound **10*EE***, in which permethylated cyclodextrins (α-CD$(OMe)_{17}$) linked directly to *trans*-azobenzene units comprise the self-complementary monomers of a [*c*2]daisy chain. Irradiation at 366 nm sparingly populates the **10*EZ*** and **10*ZZ*** isomers (corresponding to $E \rightarrow Z$ photoisomerization of one or two azobenzenes), which represent 20% and 5%, respectively, of the molecular distribution in the photostationary state (PSS) in chloroform. **10*EE*** is gradually restored by thermal relaxation. The Easton group[46] has incorporated a stilbene unit into a similar nonpermethylated architecture (Figure 4b), where the high stability of stilbene isomers allows the corresponding daisy chains **11*EE***, **11*EZ***, and **11*ZZ*** to be separated chromatographically and characterized as pure compounds. The population of isomers was found to reach approximately 2:2:1 *EE*/*EZ*/*ZZ* in the PSS with irradiation at 350 nm.

Compounds **10** and **11** both supply a ~0.7 nm contraction upon photoisomerization, where the extruded α-CD rings of the *ZZ* isomers move to encircle short trimethylene chains. Harada's group prepared[47] a [*c*2]daisy chain (**12*EE***) with a long polyether spacer between its azobenzene and heptamethylene stations. Under irradiation, the *Z* conformation of azobenzene is populated at 40% and 85% ratios in water and methanol, respectively, in the PSS. Although the extended length of **12*EE*** and **12*ZZ*** vastly exceeds that of **10** and **11**, the high flexibility of the polyether

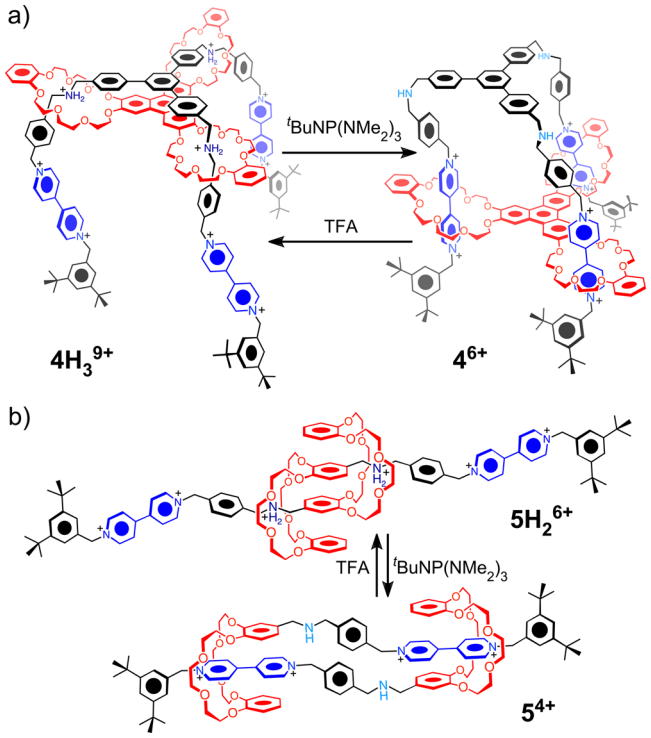

Figure 2. Two examples of pH-switchable molecular muscles based on dialkylammonium and bipyridinium recognition sites with crown ether rings. (a) Actuation of molecular elevator $\mathbf{4H_3}^{9+}/\mathbf{4}^{6+}$. (b) Actuation of [*c*2]daisy chain $\mathbf{5H_2}^{6+}/\mathbf{5}^{4+}$.

chains reduces the effective contraction length. The hydrodynamic radius (R_H) in water is shortened from 4.4 nm in **12*EE*** to 3.6 nm in **12*ZZ***. [*c*2]Daisy chains should therefore incorporate rigid rods, if possible, to maximize the extent of contraction/expansion.

SOLVENT-DRIVEN SWITCHING

Changes in solvent polarity (Figure 5) are effective handles on rotaxanes because they influence local noncovalent interactions. An example (Figure 5a) of an explicitly solvent-switchable rotaxane muscle is daisy chain **13**, a predecessor of **12*EE***. Harada et al.[48] found that the α-CD rings of **13** encircle the appended cinnamamide units in CD_3SOCD_3, but migrate further away upon the addition of water to shield a peripheral hexamethylene chain from the more polar medium, affording a net contraction.

A descendent of Coutrot's pH-switchable daisy chain $\mathbf{6H_2}^{4+}$ is the three-station compound[49] $\mathbf{14Boc_2}^{2+}$, which can be actuated (Figure 5b) with several stimuli, including covalent modification, pH, temperature, and solvent. When exercised as a solvent-driven switch, the interior dialkylammonium centers are deactivated with *tert*-butoxycarbonyl (Boc) protecting groups, and the dibenzo[24]crown-8 rings exchange rapidly between triazolium and pyridinium stations. The authors found that the pyridinium unit is favored (88.5%) in $CDCl_3$, whereas the triazolium claims most of the crown's stabilization (97.5%) in CD_3SOCD_3.

The Huang group[50] has described (Figure 5c) the solvent-switchable pillar[5]arene-based [*c*2]daisy chain **15**, wherein a competition between dispersion forces and solvent interactions engenders mechanostereochemical sensitivity to solvent composition. With no well-defined recognition sites on its hydrocarbon chains, the statistically averaged location of the pillar[5]arene rings are near the urea-linked stopper in neat $CDCl_3$ and near the middle of the hydrocarbon chain in neat CD_3SOCD_3. The rings reside between these two positions (on average) in binary

dx.doi.org/10.1021/ar500138u | *Acc. Chem. Res.* 2014, 47, 2186−2199

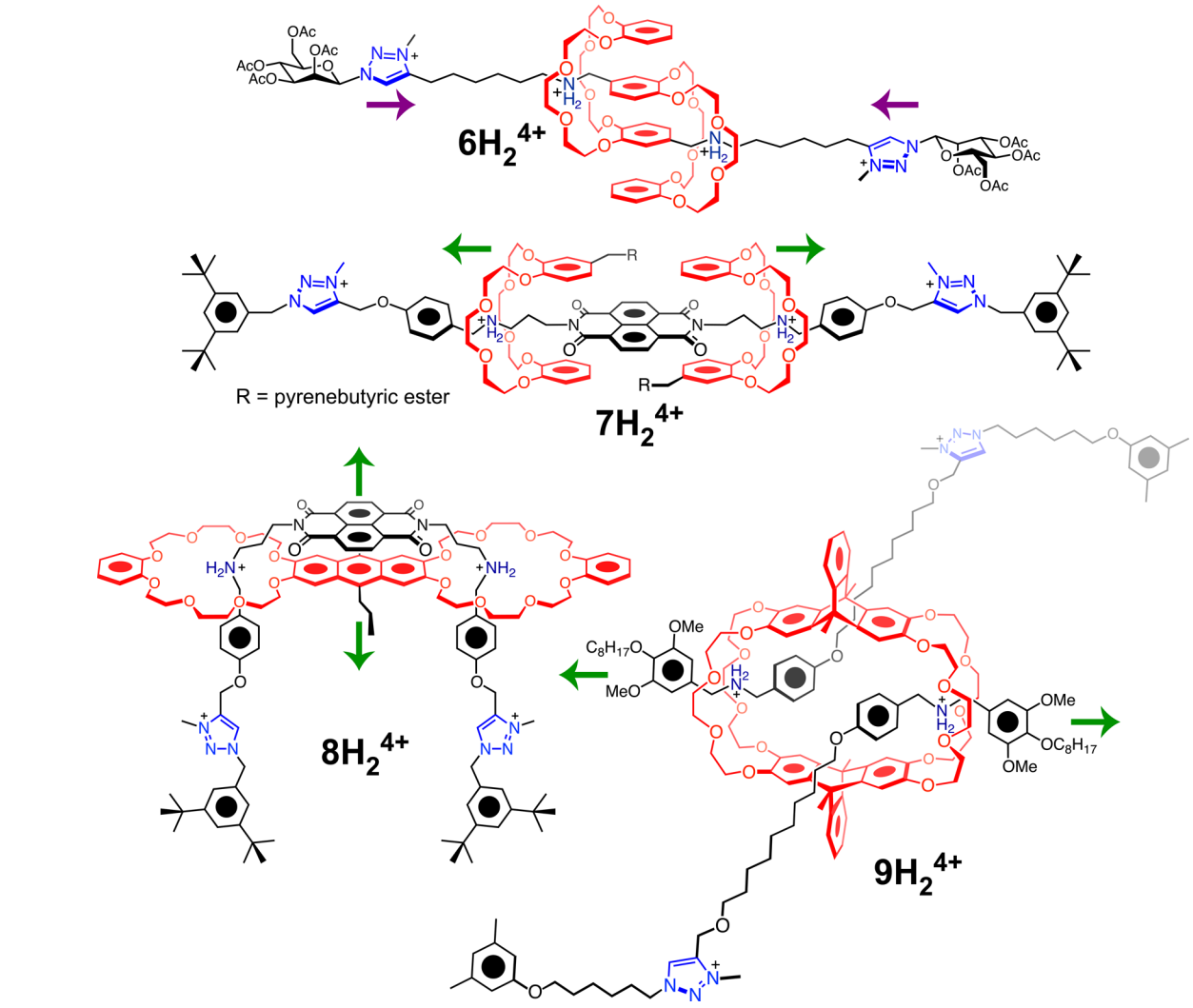

Figure 3. Four examples of pH-switchable rotaxane-based molecular muscles that utilize dialkylammonium and triazolium recognition sites with crown ether rings. Expansion or contraction (denoted by green and violet arrows, respectively) is caused by base-triggered deprotonation of the dialkylammonium groups.

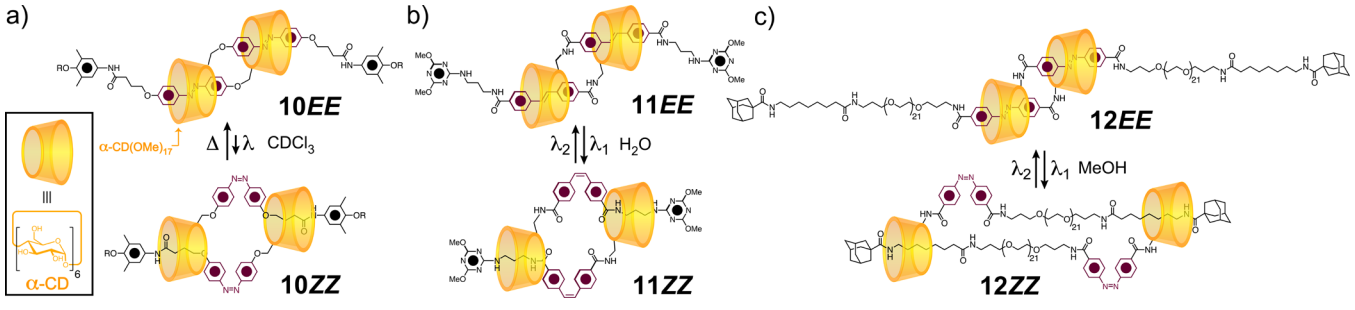

Figure 4. Photoswitchable [*c*2]daisy chains based on α-CD. (a) Actuation of **10*EE*/10*ZZ*** (λ = 366 nm). (b) Actuation of **11*EE*/11*ZZ*** (λ_1 = 350 nm, λ_2 = 254 nm). (c) Actuation of **12*EE*/12*ZZ*** (λ_1 = 365 nm, λ_2 = 430 nm).

solvents thereof. The continuous nature of this actuation scheme mimics that of the sarcomere more closely than the two-state scenario of most bistable switches.

REDOX-DRIVEN SWITCHING

We have focused our attention for two decades now on redox-switchable donor–acceptor MIMs. We first began incorporating[51−53] this technology into molecular muscles in the form of palindromic [3]rotaxanes. Within the past year, however, we have developed[54,55] (Figure 6) both neutral and cationic redox-switchable donor–acceptor daisy chains.

The neutral[54] [*c*2]daisy chain **16** comprises crown ethers with electron-rich 1,5-dioxynaphthalene (DNP) and resorcinol units, which are attached to threads bearing electron-poor naphthalene diimide (NDI) and triazole stations. Although the distribution of isomers is sensitive to temperature, the rings encircle the NDI units almost exclusively at room temperature. Daisy chain **16** is actuated (Figure 6a) by reducing electrochemically the NDI

dx.doi.org/10.1021/ar500138u | *Acc. Chem. Res.* 2014, 47, 2186−2199

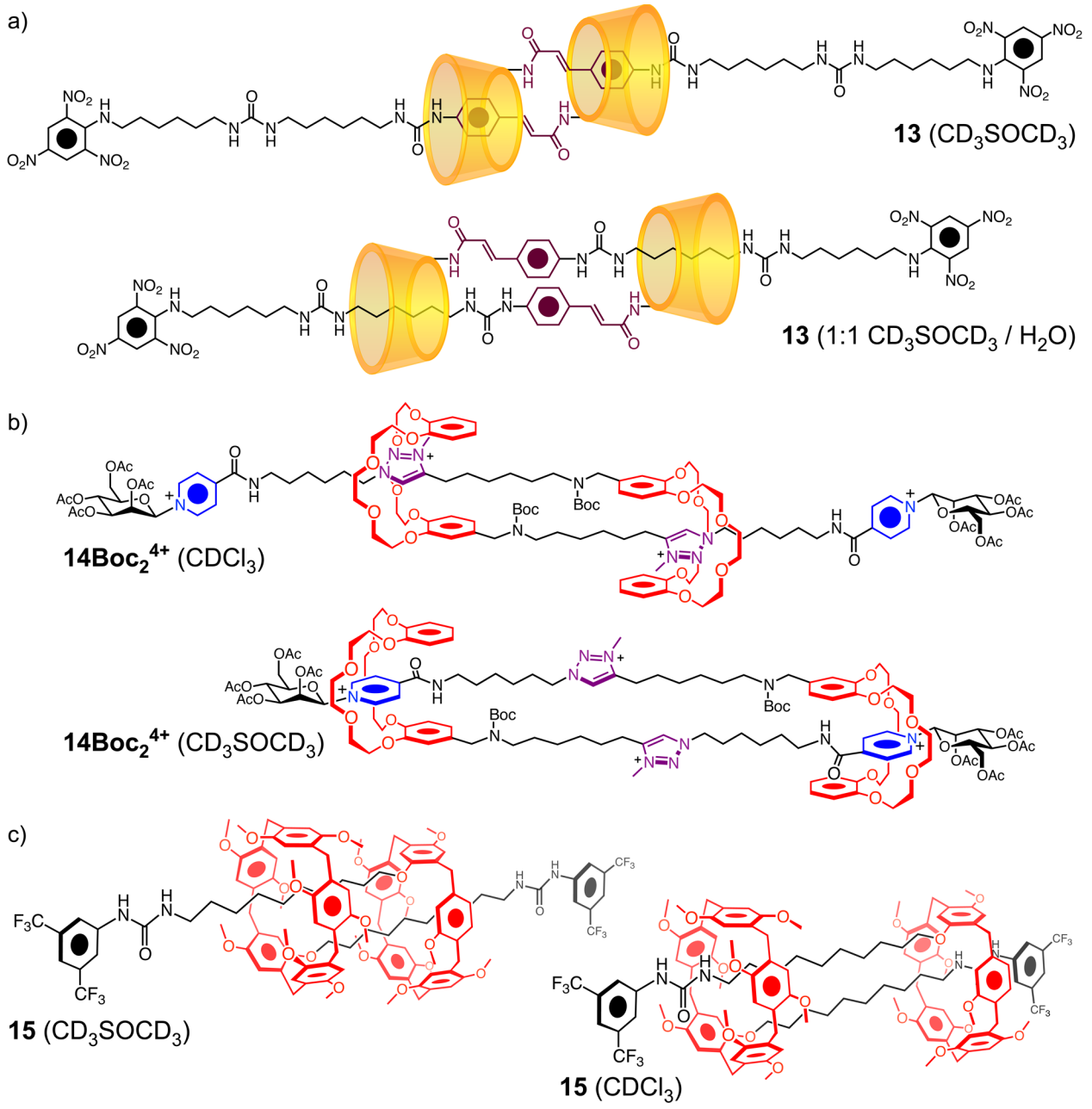

Figure 5. Prevailing coconformations of [*c*2]daisy chains **13** (a), $\mathbf{14Boc_2}^{4+}$ (b), and **15** (c) in different solvent systems.

units to the corresponding radical anions ($NDI^{\bullet-}$ or $NDI^{2(\bullet-)}$), a redox process that diminishes their electron deficiency and causes the daisy chain to contract such that its rings preferentially encircle the triazole groups in $\mathbf{16}^{4(\bullet-)}$.

The multicationic [*c*2]daisy chain $\mathbf{17}^{12+}$ is one member (Figure 6b) of a family[55] of related cyclic and acyclic daisy chains isolated from a one-pot click reaction in low yield, whose actuation is enabled by radical−radical interactions. The rings are derived from cyclobis(paraquat-*p*-phenylene) ($CBPQT^{4+}$), which has two redox-active $BIPY^{2+}$ units, while each thread carries a DNP station and another $BIPY^{2+}$ unit. Thus, $\mathbf{17}^{12+}$ is not bistable in the ground state because the $CBPQT^{4+}$ rings associate exclusively with DNP on account of repulsive Coulombic interactions between $BIPY^{2+}$ units in the rings and threads. Under reducing conditions, however, all six of the $BIPY^{\bullet+}$ radical cations (each generated in a one-electron reduction process) become associated through spin-pairing interactions in $\mathbf{17}^{6(\bullet+)}$, such that the $BIPY^{\bullet+}$ stations of the threads occupy the space in between the $BIPY^{\bullet+}$ units of $CBPQT^{2(\bullet+)}$, corresponding to an expansion in molecular length.

INTEGRATING AND SCALING FORCE AND MOTION

The stage is set for making machines out of rotaxane-based molecular muscles by coupling, integrating, and scaling up their motions. In this section, we highlight progress on garnering function from rotaxane-based muscles across length scales.

On a molecular scale, the ability of bistable rotaxanes to control mechanically the distance between two components can be exploited to tune electronic communication between chromophores. The pH-controlled quadruply interlocked molecular elevator $\mathbf{18H_8}^{4+}$ from Tanaka's group[56] demonstrates (Figure 7a) this concept. The Cu^{II} porphyrin rig has only one

dx.doi.org/10.1021/ar500138u | *Acc. Chem. Res.* 2014, 47, 2186−2199

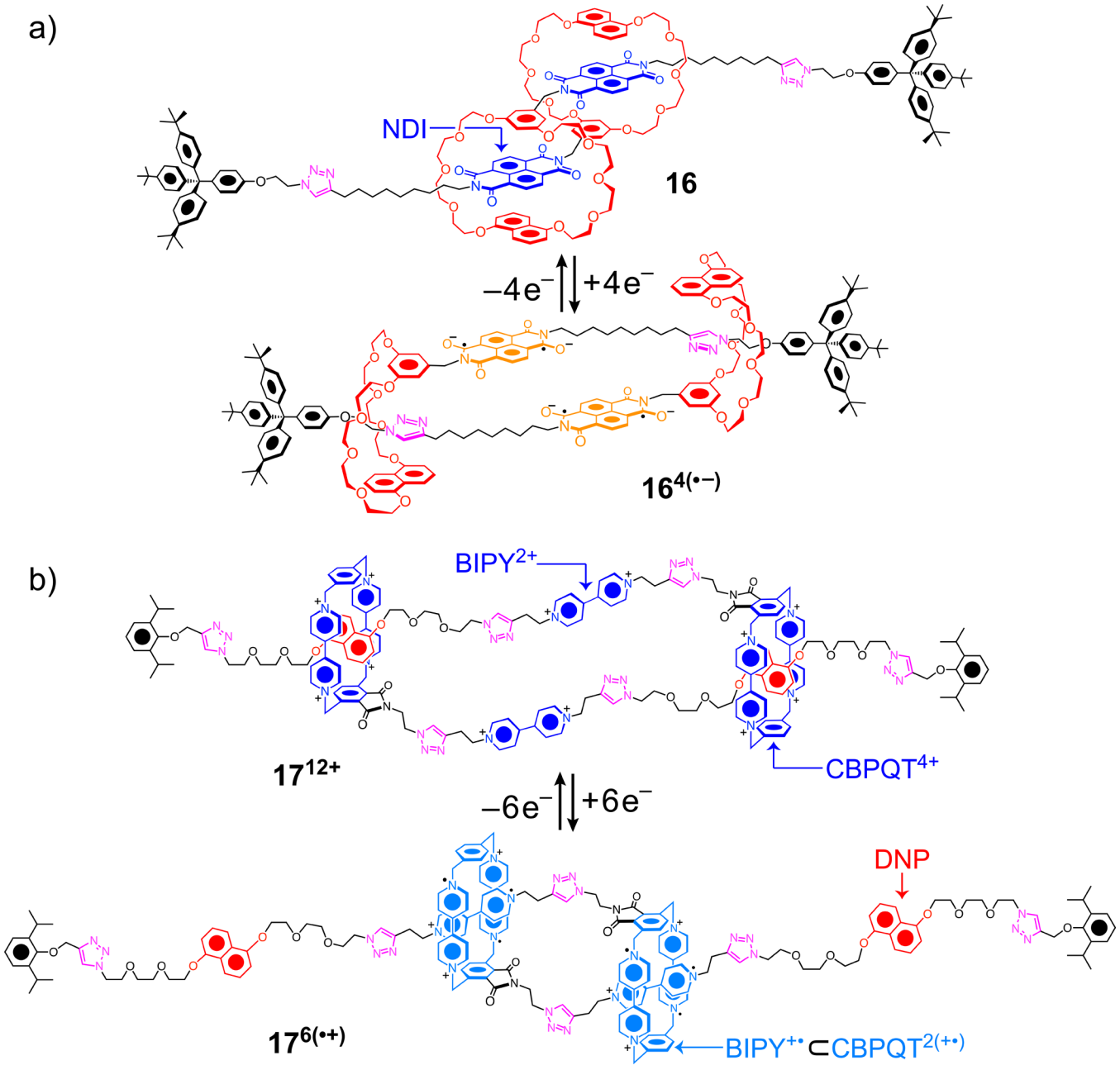

Figure 6. Redox-switchable donor–acceptor [*c*2]daisy chains. (a) Electrochemically driven actuation of neutral [*c*2]daisy chain **16**. (b) Electrochemically driven actuation of a cationic [*c*2]daisy chain, where donor–acceptor interactions underpin the contracted state of $\mathbf{17}^{12+}$ and spin-pairing interactions between $BIPY^{\bullet+}$ radicals underpin the extended state of $\mathbf{17}^{6(\bullet+)}$.

dialkylammonium recognition site on each of its four legs for the crown ethers of a Cu^{II} phthalocyanine tetramacrocycle. The authors showed by electron paramagnetic resonance spectroscopy that the phthalocyanine and porphyrin platforms establish electronic communication in $\mathbf{18}^{4-}$, a species generated by extracting four protons from the $-NH_2^+-$ centers and four protons from the phosphoramidate stoppers with a phosphazine base, since the Cu^{II} centers participate in spin-exchange interactions only in $\mathbf{18}^{4-}$ and not in $\mathbf{18H_8}^{4+}$. Note that pH-controlled movement in $\mathbf{7H_2}^{4+}$[36] and $\mathbf{8H_2}^{4+}$[37] also influences electronic communication between chromophores.

An application of rotaxane muscles as adjustable receptors has been championed by Sauvage's group.[28] The examples[57,58] portrayed in Figure 7b are complexes of a palindromic [3]rotaxane with two porphyrinic plates that act as receptors for ditopic guests. Rotaxanes **19** and $\mathbf{19Cu_2}^{2+}$ (afforded by demetalation/remetalation with Cu^{I}, respectively) express different binding properties ascribable to their mechanical geometries. Whereas the association of a 4,4′-bipyridine (BIPY) guest is greater in $\mathbf{19Cu_2}^{2+}$ (log K = 6.8) than in **19** (log K = 6.0), a longer 1,10-bis(4-pyridyl)decane (C_{10}BIPY) guest favors the more flexible rotaxane **19** (log K = 7.5) over $\mathbf{19Cu_2}^{2+}$ (log K = 6.8). An interesting future prospect for rotaxane receptors is to perform work on the guests, for example, by forcing them to adopt unfavorable conformations that store the energy associated with the mechanical stroke of the molecular muscle.

An approach (Figure 8) that we have taken toward the concerted actuation of molecular muscles is to immobilize them

dx.doi.org/10.1021/ar500138u | *Acc. Chem. Res.* 2014, 47, 2186–2199

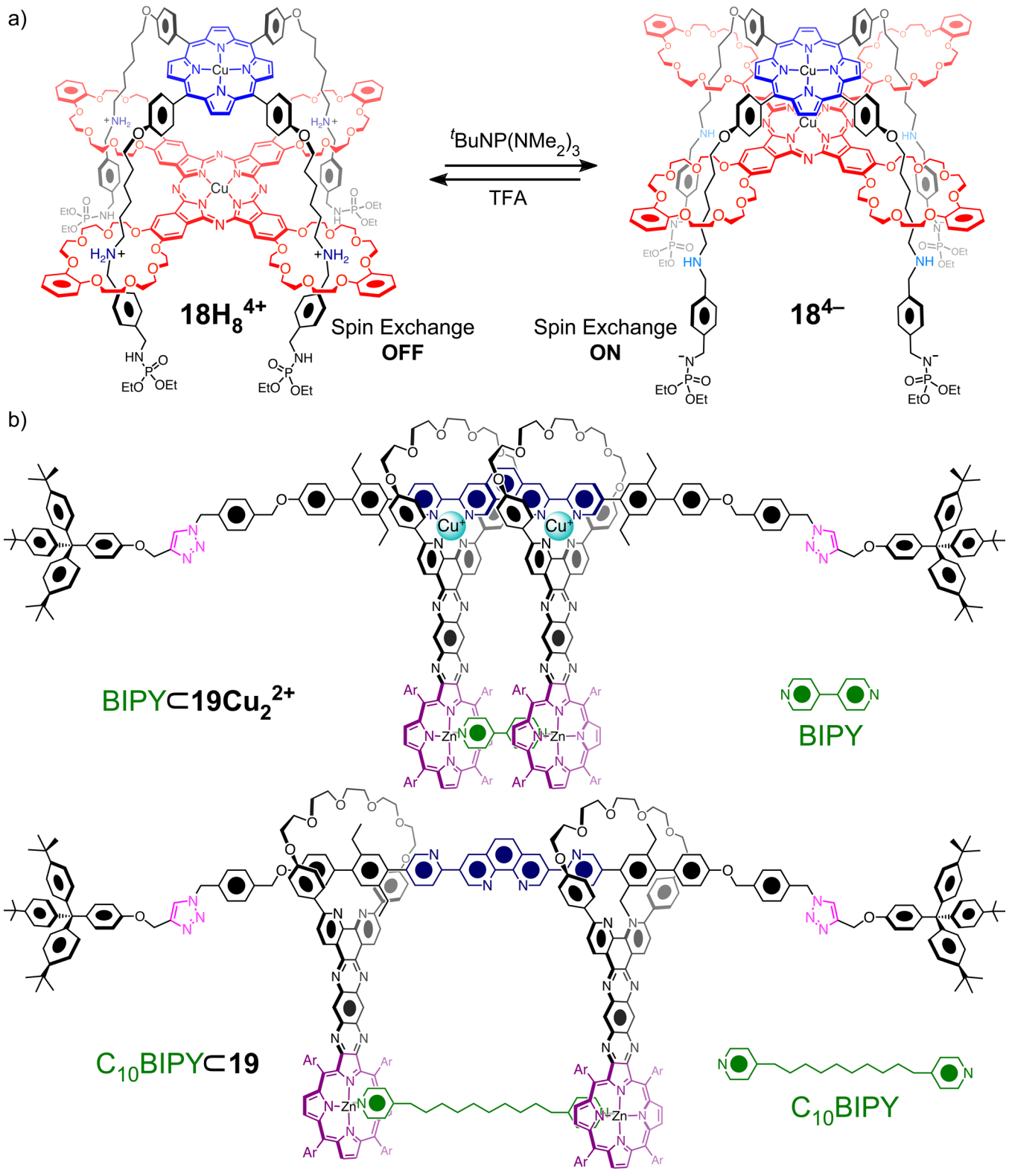

Figure 7. Applications of press rotaxanes on the molecular scale. (a) pH-Controlled platform movement in molecular elevator $\mathbf{18H_8}^{4+}/\mathbf{18}^{4-}$ influences electronic communication between the Cu^{II} centers of the porphyrin and phthalocyanine platforms. (b) Controlled ring sliding in the palindromic [3]rotaxane receptor $\mathbf{19Cu_2}^{2+}/\mathbf{19}$ influences the association of ditopic guests.

on surfaces.[51−53] The palindromic [3]rotaxane $\mathbf{20}^{8+}$ has two $CBPQT^{4+}$ rings, which preferentially encircle the dumbbell's peripheral tetrathiafulvalene (TTF) units over the DNP units near the dumbbell's center (Figure 8a). Rotaxane $\mathbf{20}^{8+}$ was deposited on one side of a gold microcantilever as a monolayer of ~8 billion molecules using disulfide tethers on the $CBPQT^{4+}$ rings. When $\mathbf{20}^{12+}$ is generated by oxidizing (Figure 8b) the TTF units to TTF^{2+} dications, the movement of the $CBPQT^{4+}$ rings toward the DNP units causes the surface to bend, as detected (Figure 8c) by a laser beam focused on the cantilever. Reduction

dx.doi.org/10.1021/ar500138u | Acc. Chem. Res. 2014, 47, 2186−2199

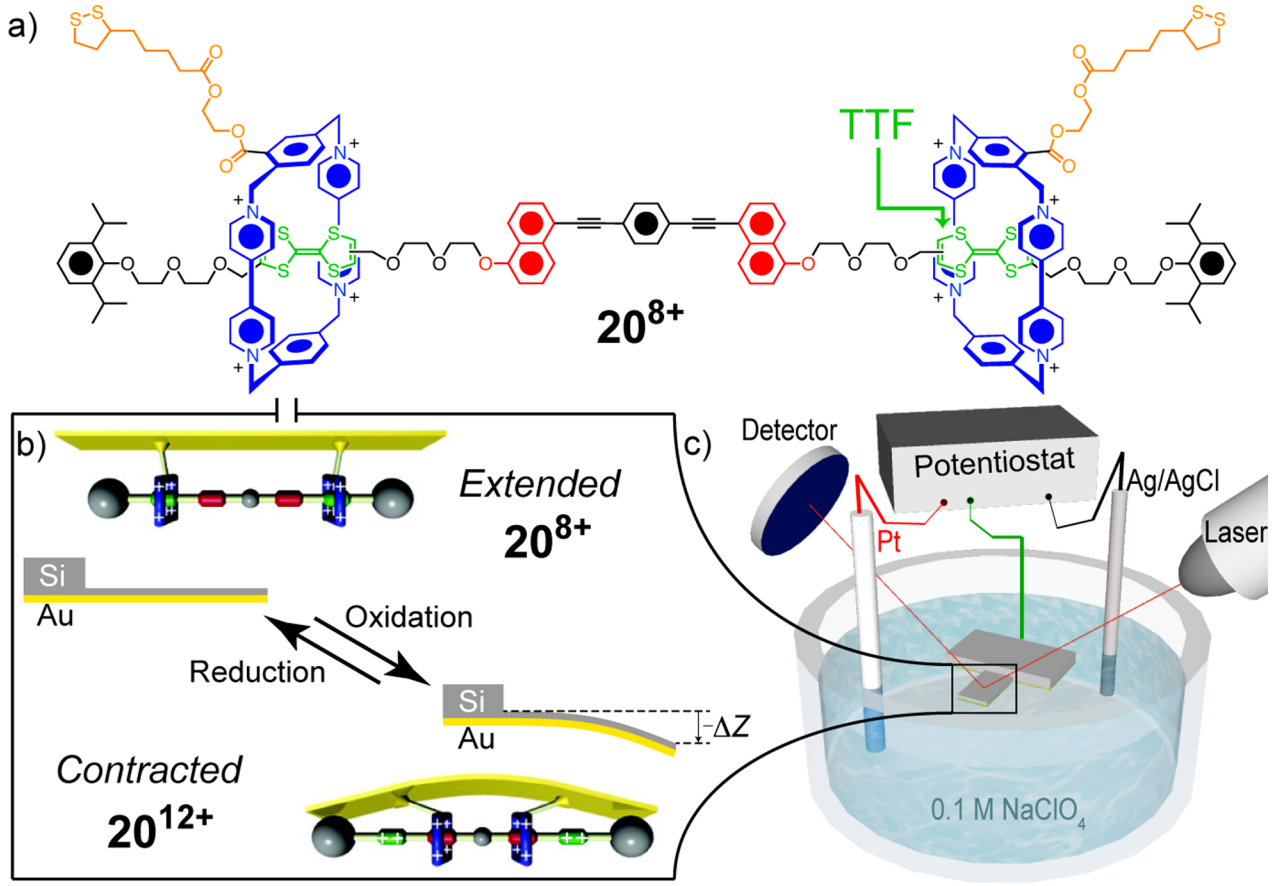

Figure 8. Bending a microcantilever with redox-switchable palindromic [3]rotaxanes. (a) Structural formula of $\mathbf{20}^{8+}$. (b) Electrochemical actuation of a monolayer of the rotaxanes immobilized on one side of a gold microcantilever. (c) Diagram of the experimental setup that detects the cantilever's bending motion with a laser.

of the TTF units back to their neutral state returns the cantilever to its former position. These redox stimuli have been introduced by both chemical[51,52] and electrochemical[53] methods.

Thousands to millions of sarcomeres are linked together in linear arrays (myofibrils) and bundled in tubular cells (myocytes). This hierarchical organization, which scales up the synchronized tiny contractions of sarcomeres, motivates the pursuit of polyrotaxanes as artificial muscles. Poly[*c*2]daisy chains (Table 1) have been the main players in this game. A major limitation is that most poly[*c*2]daisy chains have only reached low degrees of polymerization. Kaneda's group[45] attempted to polymerize **12*EE*** by connecting its terminal amide groups with *p*-xylyl linkers, affording only a pentamer as the largest product. Our attempts[59,60] to polymerize a derivative of $\mathbf{5H_2}^{6+}$ using the Cu^{I}-catalyzed azide–alkyne cycloaddition (CuAAC) yielded polymers ($\mathbf{21H_{2}}_{n}^{6n+}$) with an average of only 11 repeating units. Despite their modest size, we showed that quantitative, concerted actuation is indeed achievable along a polymer backbone. Remarkably, the base-triggered contraction ($\mathbf{21H_{2}}_{n}^{6n+} \rightarrow \mathbf{21}^{4n+}$) and acid-triggered extension ($\mathbf{21}^{4n+} \rightarrow \mathbf{21H_{2}}_{n}^{6n+}$) are faster in the polymer than in the corresponding monomer. Grubbs and co-workers[61] used CuAAC to obtain $\mathbf{22H_{2}}_{n}^{2n+}$, a dialkylammonium/crown ether poly[*c*2]daisy chain with ~22 repeating units, which extends in solution by acylation of the $-NH_2^+-$ centers to generate $\mathbf{22Ac_{2}}_{n}$. In a recent breakthrough made by the groups of Buhler and Giuseppone,[62] a metallosupramolecular approach was used to finally achieve poly[*c*2]daisy chains of high molecular weight. Their polymers $\mathbf{23Fe}_n\mathbf{H_{2}}_{n}^{6n+}$ and $\mathbf{23Fe}_n^{4n+}$ are derived from Coutrot's daisy chain $\mathbf{6H_2}^{4+}/\mathbf{6}^{2+}$, with terpyridine ligands serving as stoppers. The ligands dimerize around Fe^{II} ions during the metallosupramolecular polymerization to afford linear polymers with an average of ~3000 repeating units. The authors proved[62,63] the potential of long poly[*c*2]daisy chains to amplify the nanomotions of rotaxanes over several orders of magnitude, since the contour lengths of $\mathbf{23Fe}_n\mathbf{H_{2}}_{n}^{6n+}$ (15.9 μm) and $\mathbf{23Fe}_n^{4n+}$ (9.4 μm) differ by 6.5 μm.

Quantitative estimates of the contraction distances for the molecular muscles discussed in this Account are tabulated in Table 2. Most of the estimates are based on measurements made *in silico* by the authors or ourselves, although some of the values have been measured experimentally. High molecular weight polymers of rotaxane-based molecular muscles have moved us one step closer to macroscopic artificial muscles. We can only speculate on the advantageous properties these polymers might possess, but it stands to reason that the extra entropy afforded by mechanical ring sliding could impart rotaxane-based artificial muscles with remarkable viscoelastic properties, as observed[64] in polyrotaxane slide-ring gels.

Having addressed the *motions* of rotaxane-based molecular muscles, we now consider the *forces* generated by bistable rotaxanes. Force measurements on individual [2]rotaxanes have been performed[65,66] using atomic force microscopy (AFM) by immobilizing the dumbbell on a surface and tethering the ring to an AFM cantilever. A collaboration[65] among our group and those of Houk and Ho at UCLA allowed us to evaluate the actuation

dx.doi.org/10.1021/ar500138u | *Acc. Chem. Res.* 2014, 47, 2186–2199

Table 1. Summary of pH-Switchable Poly[*c*2]Daisy Chains

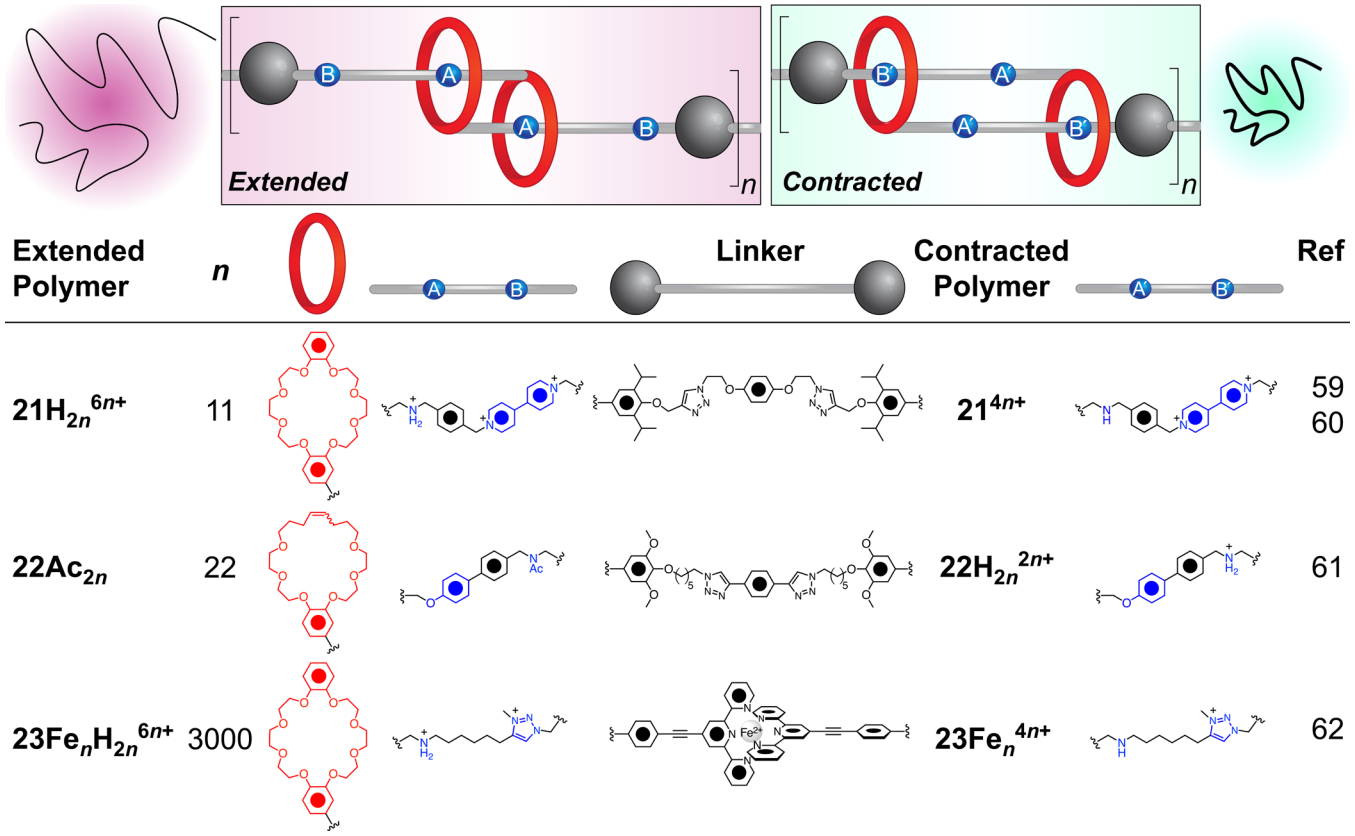

Table 2. Metrics of Contractile/Extensile Motions in Rotaxane-Based Molecular Muscles

extended state	extended length (nm)	contracted state	contracted length (nm)	contraction distance (nm)	contraction ratio[a] (%)	stimulus	ref
$\mathbf{1Cu_2}^{2+}$	8.3	$\mathbf{1Zn_2}^{4+}$	6.5	1.8	22	cations	25, 26
$\mathbf{2Cu_4}^{4+}$	4.6	**2**	1.9	2.7	59	cations	29, 30
3·4PF_6	4.0	**3**·4F	2.5	1.5	38	anions	31
$\mathbf{4}^{6+}$	1.1	$\mathbf{4H_3}^{9+}$	0.4	0.7	64	pH	32, 33
$\mathbf{5H_2}^{6+}$	3.1	$\mathbf{5}^{4+}$	2.2	0.9	29	pH	34
$\mathbf{6H_2}^{4+}$	4.2	$\mathbf{6}^{2+}$	3.0	1.2	29	pH	35
$\mathbf{7}^{2+}$	3.1	$\mathbf{7H_2}^{4+}$	1.6	1.5	48	pH	36
$\mathbf{8}^{2+}$	1.2	$\mathbf{8H_2}^{4+}$	0.4	0.8	67	pH	37
$\mathbf{9}^{2+}$	7.7	$\mathbf{9H_2}^{4+}$	3.2	4.5	58	pH	38
10*EE*	3.0	**10*ZZ***	2.3	0.7	23	*hν*	45
11*EE*	3.0	**11*ZZ***	2.3	0.7	23	*hν*	46
12*EE*	8.8[b]	**12*ZZ***	7.2[b]	1.6	18	*hν*	47
13 (CD_3SOCD_3)		**13** (H_2O)		0.7		solvent	48
$\mathbf{14Boc_2}^{4+}$ ($CDCl_3$)	5.4	$\mathbf{14Boc_2}^{4+}$ (CD_3SOCD_3)	4.4	1.0	19	solvent	49
15 (CD_3SOCD_3)	3.7	**15** ($CDCl_3$)	3.1	0.6	16	solvent	50
16	5.2	$\mathbf{16}^{4(\bullet-)}$	3.4	1.8	35	redox	54
$\mathbf{17}^{6(\bullet+)}$	10.1	$\mathbf{17}^{12+}$	6.7	3.4	34	redox	55
$\mathbf{18H_8}^{4+}$	0.9	$\mathbf{18}^{4-}$	0.4	0.5	56	pH	56
BC_{10}PY⊂**19**	1.8	BIPY⊂$\mathbf{19Cu_2}^{2+}$	0.8	1.0	56	cations	57, 58
$\mathbf{20}^{8+}$	4.2	$\mathbf{20}^{12+}$	1.4	2.8	67	redox	51−53
$\mathbf{21H_{2n}}^{6n+}$	5.1[c]	$\mathbf{21}^{4n+}$				pH	59, 60
$\mathbf{22Ac_{2n}}$	42.8[c]	$\mathbf{22H_{2n}}^{2n+}$	29.6[c]	13.2	31	acylation	61
$\mathbf{23Fe_nH_{2n}}^{6n+}$	15900[d]	$\mathbf{23Fe_n}^{4n+}$	9400[d]	6500	41	pH	62

[a]Contraction ratio = (contraction distance/extended length) = 1 − (contracted length/extended length). [b]Reported value is twice the measured R_H, corresponding to a hydrodynamic diameter. [c]Reported value is twice the radius of gyration, R_g. [d]Countour length.

energetics of $\mathbf{24}^{4+}$, a redox-switchable donor−acceptor [2]rotaxane based on the same chemistry as that of $\mathbf{20}^{8+}$. In a pulling experiment (Figure 9), we found that much less force is required on average to pull the cyclophane off of the dumbbell in $\mathbf{24}^{4+}$ (66 pN) than in

dx.doi.org/10.1021/ar500138u | *Acc. Chem. Res.* 2014, 47, 2186−2199

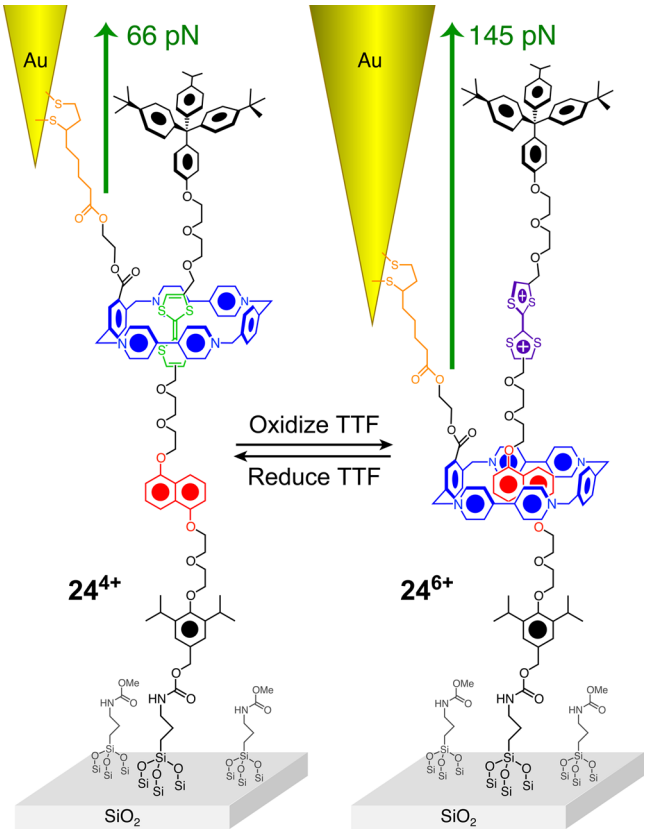

Figure 9. Force required to pull a $CBPQT^{4+}$ ring tethered to an AFM tip over the stopper of a SiO_2-immobilized dumbbell is lower (66 pN) in $\mathbf{24}^{4+}$ than in $\mathbf{24}^{6+}$ (145 pN) because of repulsive Coulombic forces, indicating that the displacement of the $CBPQT^{4+}$ ring caused by the oxidation of TTF in $\mathbf{24}^{4+}$ can generate up to 79 pN of force.

$\mathbf{24}^{6+}$ (145 pN), implying that the force associated with the electrostatically driven movement of the $CBPQT^{4+}$ ring away from TTF^{2+} upon oxidation could be as high as 79 pN. This force is large for a single molecule, since biological molecular machines generate forces of 5−60 pN.[67] Another AFM study[66] on one of Leigh's benzylic amide [2]rotaxanes revealed that it can generate 30 pN of force against a load, which is also remarkable, considering that the biased Brownian motion of its ring is driven only by weak hydrogen bonding interactions.

CONCLUSIONS AND OUTLOOK

Retrospection begets perspective. We look backward not only to admire what is behind us but also to see more clearly the path that leads forward. Perhaps the most visible milestones on the horizon, from our current vantage point, are macroscopic actuator materials based on polyrotaxanes. Further in the distance, we may find these materials in microscopic or soft robotics or sophisticated fluidic devices in which they are used to control the flow of liquids through the opening and closing of valves or the constriction and dilation of channels. An important motivation for the continued development of these rotaxanes is the remarkable diversity of molecular recognition motifs and stimuli that can be utilized in their design. Any generalizable application of rotaxanes as molecular machines that emerges in the future will benefit from this feature, owing to the different strengths of each motif in different contexts. For example, solvent switchable rotaxanes are well-suited for flow environments such as microfluidic devices, whereas electrochemically switchable rotaxanes are a better match for robotics. The biocompatibility of cyclodextrins will make α-CD-based rotaxanes more important in biological applications, whereas the structural rigidity and kinetic stability of Sauvage's[68] transition metal rotaxanes make them excellent choices for single-molecule applications. The bottom line? Rotaxanes constitute a uniquely customizable platform for directing force and motion across length scales.

AUTHOR INFORMATION

Corresponding Author

*Professor J. Fraser Stoddart. Tel: (+1)-847-491-3793. Fax: (+1)-847-491-1009. E-mail: stoddart@northwestern.edu.

Notes

The authors declare no competing financial interest.

Biographies

Carson J. Bruns received a B.A. in Chemistry and Religion from Luther College in 2008, and a Ph.D. in Organic Chemistry from Northwestern University in 2013 under the supervision of Professors Fraser Stoddart and Samuel Stupp. His research involves donor−acceptor molecules that transduce energy. Later this year, he will join the Francis group at the University of California, Berkeley, as a Miller Fellow.

J. Fraser Stoddart received B.Sc., Ph.D., and D.Sc. Degrees from the University of Edinburgh. He currently holds a Board of Trustees Professorship in the Department of Chemistry at Northwestern University. His research in molecular nanotechnology involves the synthesis and self-assembly of supramolecular and mechanically interlocked compounds and their applications in new materials and technologies.

ACKNOWLEDGMENTS

We thank the Joint Center of Excellence in Integrated Nano-Systems (JCIN) at King Abdul-Aziz City for Science and Technology (KACST) and Northwestern University (NU) for supporting this research (Projects 34-947 and 34-948) and the Non-Equilibrium Energy Research Center (NERC), an Energy Frontiers Research Center (EFRC) funded by the U.S. Department of Energy, Office of Science, Office of Basic Energy Sciences under Award DE-SC0000989.

REFERENCES

(1) Barabási, A.-L.; Oltvai, Z. N. Network Biology: Understanding the Cell's Functional Organization. *Nature Rev. Genet.* **2004**, *5*, 101−113.
(2) Alberts, B. The Cell as a Collection of Protein Machines: Preparing the Next Generation of Molecular Biologists. *Cell* **1998**, *92*, 291−294.
(3) Alberts, B.; Johnson, A.; Lewis, J.; Raff, M.; Roberts, K.; Walter, P. *Molecular Biology of the Cell*, 5th ed.; Garland Science: New York, 2008.
(4) Balzani, V.; Credi, A.; Raymo, F.; Stoddart, J. F. Artificial Molecular Machines. *Angew. Chem., Int. Ed.* **2000**, *39*, 3348−3391.
(5) Kay, E. R.; Leigh, D. A.; Zerbetto, F. Synthetic Molecular Motors and Mechanical Machines. *Angew. Chem., Int. Ed.* **2007**, *46*, 72−191.
(6) Coskun, A.; Banaszak, M.; Astumian, R. D.; Stoddart, J. F.; Grzybowski, B. A. Great Expectations: Can Artificial Molecular Machines Deliver on Their Promise? *Chem. Soc. Rev.* **2012**, *41*, 19−30.
(7) Stoddart, J. F. The Chemistry of the Mechanical Bond. *Chem. Soc. Rev.* **2009**, *38*, 1802−1820.
(8) Olson, M. A.; Botros, Y. Y.; Stoddart, J. F. Mechanostereochemistry. *Pure Appl. Chem.* **2010**, *82*, 1569−1574.
(9) Browne, W. R.; Feringa, B. L. Making Molecular Machines Work. *Nature Nanotech.* **2006**, *1*, 25−35.
(10) Eelkema, R.; Pollard, M.; Vicario, J.; Katsonis, N.; Ramon, B.; Bastiaansen, C. W. M.; Broer, D. J.; Feringa, B. L. Nanomotor Rotates Microscale Objects. *Nature* **2006**, *440*, 163−163.

(11) Berná, J.; Leigh, D. A.; Lubomska, M.; Mendoza, S. M.; Pérez, E. M.; Rudolf, P.; Teobaldi, G.; Zerbetto, F. Macroscopic Transport by Synthetic Molecular Machines. *Nature Mater.* **2005**, *4*, 704−710.
(12) Yamada, M.; Kondo, M.; Mamiya, J.-I.; Yu, Y.; Kinoshita, M.; Barrett, C. J.; Ikeda, T. Photomobile Polymer Materials: Towards Light-Driven Plastic Motors. *Angew. Chem., Int. Ed.* **2008**, *47*, 4986−4988.
(13) Iamsaard, S.; Aßhoff, S. J.; Matt, B.; Kudernac, T.; Cornelissen, J. J. L. M.; Fletcher, S. P.; Katsonis, N. Conversion of Light into Macroscopic Helical Motion. *Nature Chem.* **2014**, *6*, 229−235.
(14) Mirfakhrai, T.; Madden, J. D.; Baughman, R. H. Polymer Artificial Muscles. *Mater. Today* **2007**, *10*, 30−38.
(15) Brochu, P.; Pei, Q. Advances in Dielectric Elastomers for Actuators and Artificial Muscles. *Macromol. Rapid Commun.* **2010**, *31*, 10−36.
(16) Osada, Y. Conversion of Chemical into Mechanical Energy by Synthetic Polymers. *Adv. Polym. Sci.* **1987**, *82*, 1−46.
(17) Baughman, R. H. Conducting Polymer Artificial Muscles. *Synth. Met.* **1996**, *78*, 339−353.
(18) Lendlein, A.; Kelch, S. Shape-Memory Polymers. *Angew. Chem., Int. Ed.* **2002**, *41*, 2034−2057.
(19) Ikeda, T.; Mamiya, J.-I.; Yu, Y. Photomechanics of Liquid-Crystalline Elastomers and Other Polymers. *Angew. Chem., Int. Ed.* **2007**, *46*, 506−528.
(20) Wei, J.; Yu, Y. Photodeformable Polymer Gels and Crosslinked Liquid-Crystalline Polymers. *Soft Matter* **2012**, *8*, 8050−8059.
(21) Takashima, Y.; Hatanaka, S.; Otsubo, M.; Nakahata, M.; Kakuta, T.; Hashidzume, A.; Yamaguchi, H.; Harada, A. Expansion-Contraction of Photoresponsive Artificial Muscle Regulated by Host-Guest Interactions. *Nature Commun.* **2012**, *3*, 1270−1278.
(22) Irie, M. Photochromism and Molecular Mechanical Devices. *Bull. Chem. Soc. Jpn.* **2008**, *81*, 917−926.
(23) Ballardini, R.; Balzani, V.; Credi, A.; Gandolfi, M. T.; Venturi, M. Artificial Molecular-Level Machines: Which Energy to Make Them Work? *Acc. Chem. Res.* **2001**, *34*, 445−455.
(24) Rotzler, J.; Mayor, M. Molecular Daisy Chains. *Chem. Soc. Rev.* **2013**, *42*, 44−62.
(25) Jiménez, M. C.; Dietrich-Buchecker, C.; Sauvage, J.-P. Towards Synthetic Molecular Muscles: Contraction and Stretching of a Linear Rotaxane Dimer. *Angew. Chem., Int. Ed.* **2000**, *39*, 3284−3287.
(26) Jimenez-Molero, M.; Dietrich-Buchecker, C.; Sauvage, J.-P. Chemically Induced Contraction and Stretching of a Linear Rotaxane Dimer. *Chem.—Eur. J.* **2002**, *8*, 1456−1466.
(27) Jimenez-Molero, M. C.; Dietrich-Buchecker, C.; Sauvage, J.-P. Towards Artificial Muscles at the Nanometric Level. *Chem. Commun.* **2003**, 1613−1616.
(28) Durola, F.; Heitz, V.; Reviriego, F.; Roche, C.; Sauvage, J.-P.; Sour, A.; Trolez, Y. Cyclic [4]Rotaxanes Containing Two Parallel Porphyrinic Plates: Toward Switchable Molecular Receptors and Compressors. *Acc. Chem. Res.* **2014**, *47*, 633−645.
(29) Collin, J.-P.; Durola, F.; Frey, J.; Heitz, V.; Reviriego, F.; Sauvage, J.-P.; Trolez, Y.; Rissanen, K. Templated Synthesis of Cyclic [4]Rotaxanes Consisting of Two Stiff Rods Threaded Through Two Bis-Macrocycles with a Large and Rigid Central Plate as Spacer. *J. Am. Chem. Soc.* **2010**, *132*, 6840−6850.
(30) Collin, J.-P.; Durola, F.; Heitz, V.; Reviriego, F.; Sauvage, J.-P.; Trolez, Y. A Cyclic [4]Rotaxane That Behaves as a Switchable Molecular Receptor: Formation of a Rigid Scaffold From a Collapsed Structure by Complexation with Copper(I) Ions. *Angew. Chem., Int. Ed.* **2010**, *49*, 10172−10175.
(31) Chuang, C.-J.; Li, W.-S.; Lai, C.-C.; Liu, Y.-H.; Peng, S.-M.; Chao, I.; Chiu, S.-H. A Molecular Cage-Based [2]Rotaxane That Behaves as a Molecular Muscle. *Org. Lett.* **2009**, *11*, 385−388.
(32) Badjić, J. D.; Balzani, V.; Credi, A.; Silvi, S.; Stoddart, J. F. A Molecular Elevator. *Science* **2004**, *303*, 1845−1849.
(33) Badjić, J. D.; Ronconi, C. M.; Stoddart, J. F.; Balzani, V.; Silvi, S.; Credi, A. Operating Molecular Elevators. *J. Am. Chem. Soc.* **2006**, *128*, 1489−1499.
(34) Wu, J.; Leung, K. C.-F.; Benítez, D.; Han, J.-Y.; Cantrill, S. J.; Fang, L.; Stoddart, J. F. An Acid-Base-Controllable [*c*2]Daisy Chain. *Angew. Chem., Int. Ed.* **2008**, *47*, 7470−7474.
(35) Coutrot, F.; Romuald, C.; Busseron, E. A New pH-Switchable Dimannosyl[*c*2]Daisy Chain Molecular Machine. *Org. Lett.* **2008**, *10*, 3741−3744.
(36) Jiang, Q.; Zhang, H.-Y.; Han, M.; Ding, Z.-J.; Liu, Y. pH-Controlled Intramolecular Charge-Transfer Behavior in Bistable [3]Rotaxane. *Org. Lett.* **2010**, *12*, 1728−1731.
(37) Zhang, Z.-J.; Han, M.; Zhang, H.-Y.; Liu, Y. A Double-Leg Donor-Acceptor Molecular Elevator: New Insight into Controlling the Distance of Two Platforms. *Org. Lett.* **2013**, *15*, 1698−1701.
(38) Jiang, Y.; Guo, J.-B.; Chen, C.-F. A New [3]Rotaxane Molecular Machine Based on a Dibenzylammonium Ion and a Triazolium Station. *Org. Lett.* **2010**, *12*, 4248−4251.
(39) Tuncel, D.; Özsar, Ö.; Tiftik, H. B.; Salih, B. Molecular Switch Based on a Cucurbit[6]uril Containing Bistable [3]Rotaxane. *Chem. Commun.* **2007**, 1369−1371.
(40) Tuncel, D.; Katterle, M. pH-Triggered Dethreading-Rethreading and Switching of Cucurbit[6]uril on Bistable [3]Pseudorotaxanes and [3]Rotaxanes. *Chem.—Eur. J.* **2008**, *14*, 4110−4116.
(41) Nakazono, K.; Takata, T. Neutralization of a *sec*-Ammonium Group Unusually Stabilized by the "Rotaxane Effect": Synthesis, Structure, and Dynamic Nature of a 'Free' *sec*-Amine/Crown Ether-Type Rotaxane. *Chem.—Eur. J.* **2010**, *16*, 13783−13794.
(42) Yang, W.; Li, Y.; Zhang, J.; Chen, N.; Chen, S.; Liu, H.; Li, Y. A Controllable Chiral Molecular Machine: Movement on Molecular Level. *Small* **2012**, *8*, 2602−2607.
(43) Tokunaga, Y.; Ikezaki, S.; Kimura, M.; Hisada, K.; Kawasaki, T. Five-State Molecular Switching of a [3]Rotaxane in Response to Weak and Strong Acid and Base Stimuli. *Chem. Commun.* **2013**, *49*, 11749−11751.
(44) Balzani, V.; Credi, A.; Venturi, M. Light Powered Molecular Machines. *Chem. Soc. Rev.* **2009**, *38*, 1542−1550.
(45) Tsuda, S.; Aso, Y.; Kaneda, T. Linear Oligomers Composed of a Photochromically Contractible and Extendable Janus [2]Rotaxane. *Chem. Commun.* **2006**, 3072−3074.
(46) Dawson, R. E.; Lincoln, S. F.; Easton, C. J. The Foundation of a Light Driven Molecular Muscle Based on Stilbene and α-Cyclodextrin. *Chem. Commun.* **2008**, 3980−3982.
(47) Li, S.; Taura, D.; Hashidzume, A.; Harada, A. Light-Switchable Janus [2]Rotaxanes Based on α-Cyclodextrin Derivatives Bearing Two Recognition Sites Linked with Oligo(Ethylene Glycol). *Chem.—Asian J.* **2010**, *5*, 2281−2289.
(48) Tsukagoshi, S.; Miyawaki, A.; Takashima, Y.; Yamaguchi, H.; Harada, A. Contraction of Supramolecular Double-Threaded Dimer Formed by α-Cyclodextrin with a Long Alkyl Chain. *Org. Lett.* **2007**, *9*, 1053−1055.
(49) Romuald, C.; Busseron, E.; Coutrot, F. Very Contracted to Extended Co-Conformations with or Without Oscillations in Two- and Three-Station [*c*2]Daisy Chains. *J. Org. Chem.* **2010**, *75*, 6516−6531.
(50) Zhang, Z.; Han, C.; Yu, G.; Huang, F. A Solvent-Driven Molecular Spring. *Chem. Sci.* **2012**, *3*, 3026−3031.
(51) Huang, T. J.; Brough, B.; Ho, C.-M.; Liu, Y.; Flood, A. H.; Bonvallet, P. A.; Tseng, H.-R.; Stoddart, J. F.; Baller, M.; Magonov, S. A Nanomechanical Device Based on Linear Molecular Motors. *Appl. Phys. Lett.* **2004**, *85*, 5391−5393.
(52) Liu, Y.; Flood, A. H.; Bonvallet, P. A.; Vignon, S. A.; Northrop, B. H.; Tseng, H.-R.; Jeppesen, J. O.; Huang, T. J.; Brough, B.; Baller, M.; Magonov, S.; Solares, S. D.; Goddard, W. A., III; Ho, C.-M.; Stoddart, J. F. Linear Artificial Molecular Muscles. *J. Am. Chem. Soc.* **2005**, *127*, 9745−9759.
(53) Juluri, B. K.; Kumar, A. S.; Liu, Y.; Ye, T.; Yang, Y.-W.; Flood, A. H.; Fang, L.; Stoddart, J. F.; Weiss, P. S.; Huang, T. J. A Mechanical Actuator Driven Electrochemically by Artificial Molecular Muscles. *ACS Nano* **2009**, *3*, 291−300.
(54) Bruns, C. J.; Li, J.; Frasconi, M.; Schneebeli, S. T.; Iehl, J.; Jacquot de Rouville, H.-P.; Stupp, S. I.; Voth, G. A.; Stoddart, J. F. An

Electrochemically and Thermally Switchable Donor-Acceptor [*c*2]Daisy Chain Rotaxane. *Angew. Chem., Int. Ed.* **2014**, *53*, 1953−1958.
(55) Bruns, C. J.; Frasconi, M.; Iehl, J.; Hartlieb, K. J.; Schneebeli, S. T.; Cheng, C.; Stupp, S. I.; Stoddart, J. F. Redox Switchable Daisy Chain Rotaxanes Driven by Radical−Radical Interactions. *J. Am. Chem. Soc.* **2014**, *136*, 4714−4723.
(56) Yamada, Y.; Okamoto, M.; Furukawa, K.; Kato, T.; Tanaka, K. Switchable Intermolecular Communication in a Four-Fold Rotaxane. *Angew. Chem., Int. Ed.* **2012**, *51*, 709−713.
(57) Frey, J.; Tock, C.; Collin, J.-P.; Heitz, V.; Sauvage, J.-P. A [3]Rotaxane with Two Porphyrinic Plates Acting as an Adaptable Receptor. *J. Am. Chem. Soc.* **2008**, *130*, 4592−4593.
(58) Collin, J.-P.; Frey, J.; Heitz, V.; Sauvage, J.-P.; Tock, C.; Allouche, L. Adjustable Receptor Based on a [3]Rotaxane Whose Two Threaded Rings Are Rigidly Attached to Two Porphyrinic Plates: Synthesis and Complexation Studies. *J. Am. Chem. Soc.* **2009**, *131*, 5609−5620.
(59) Fang, L.; Hmadeh, M.; Wu, J.; Olson, M. A.; Spruell, J. M.; Trabolsi, A.; Yang, Y.-W.; Elhabiri, M.; Albrecht-Gary, A.-M.; Stoddart, J. F. Acid-Base Actuation of [*c*2]Daisy Chains. *J. Am. Chem. Soc.* **2009**, *131*, 7126−7134.
(60) Hmadeh, M.; Fang, L.; Trabolsi, A.; Elhabiri, M.; Albrecht-Gary, A.-M.; Stoddart, J. F. On the Thermodynamic and Kinetic Investigations of a [*c*2]Daisy Chain Polymer. *J. Mater. Chem.* **2010**, *20*, 3422−3430.
(61) Clark, P. G.; Day, M. W.; Grubbs, R. H. Switching and Extension of a [*c*2]Daisy-Chain Dimer Polymer. *J. Am. Chem. Soc.* **2009**, *131*, 13631−13633.
(62) Du, G.; Moulin, E.; Jouault, N.; Buhler, E.; Giuseppone, N. Muscle-Like Supramolecular Polymers: Integrated Motion From Thousands of Molecular Machines. *Angew. Chem., Int. Ed.* **2012**, *51*, 12504−12508.
(63) Bruns, C. J.; Stoddart, J. F. Supramolecular Polymers: Molecular Machines Muscle Up. *Nature Nanotech.* **2013**, *8*, 9−10.
(64) Ito, K. Novel Entropic Elasticity of Polymeric Materials: Why Is Slide-Ring Gel So Soft? *Polym. J.* **2012**, *44*, 38−71.
(65) Brough, B.; Northrop, B. H.; Schmidt, J. J.; Tseng, H.-R.; Houk, K. N.; Stoddart, J. F.; Ho, C.-M. Evaluation of Synthetic Linear Motor-Molecule Actuation Energetics. *Proc. Natl. Acad. Sci. U.S.A.* **2006**, *103*, 8583−8588.
(66) Lussis, P.; Svaldo-Lanero, T.; Bertocco, A.; Fustin, C.-A.; Leigh, D. A.; Duwez, A.-S. A Single Synthetic Small Molecule That Generates Force against a Load. *Nature Nanotech.* **2011**, *6*, 553−557.
(67) Bustamante, C.; Chemla, Y. R.; Forde, N. R.; Izhaky, D. Mechanical Processes in Biochemistry. *Annu. Rev. Biochem.* **2004**, *73*, 705−748.
(68) Niess, F.; Duplan, V.; Sauvage, J.-P. Molecular Muscles: From Species in Solution to Materials and Devices. *Chem. Lett.* **2014**, DOI: 10.1246/cl.140315.